resemblance between these two classes of polymers. Both classes of macromolecules possess a negatively charged, solvent-compatible, congested outer surface into which postively charged molecules can be solubilized. Our results indicate that the occupation of the molecules among these macromolecules is Poissonian in nature and their distribution on the surface is random. The exact location of solubilization, however, is not well-known at this time. The solubilized molecules are capable of diffusion on the surface and the rate of diffusion and rate of exit from the surfaces depend on the size of the macromolecule. For example, we have noted that the intramicellar quenching rate constant decreased with increase in the size of the micelle or starburst dendrimer. Quenching studies with ferrocyanide indicated that the exit of the probe is significant only in the case of the smaller micelles or dendrimers.

In summary, the flourescence probe method can be profitably employed to investigate the morphology of the starburst dendrimers and to define similarities between these systems and anionic micelles. Our studies reveal a strong resemblance between these two classes of macromolecules and also support the results of the molecular simulation studies, which predict a change in the morphology of the dendrimers at generation 3.

Acknowledgment. We thank the NSF, the DOE, the AFOSR, and the ONR for their generous support of this research. Our thanks also to Professor F. C. De Schryver for providing us with the computer program used to analyze the experimental data. A.R.L. thanks the NIH for a NRSA fellowship. D.A.T. thanks the New Energy and Development Organization (NEDO) of the Ministry of International Trade and Industry of Japan (MITI) for generous support of certain critical synthetic efforts.

Registry No. OSS, 142-31-4; DSS, 142-87-0; SDS, 151-21-3; HSS, 18981-98-1; NSS, 1072-15-7; UDS, 1072-24-8; MV^{2+}, 1910-42-5; $Ru(phen)_3^{2+}\cdot 2Cl^-$, 23570-43-6; $K_4[Fe(CN)_6]$, 13943-58-3.

Molecular Recognition at the Air–Water Interface. Specific Binding of Nitrogen Aromatics and Amino Acids by Monolayers of Long-Chain Derivatives of Kemp's Acid

Yasuhiro Ikeura, Kazue Kurihara, and Toyoki Kunitake*,†

Contribution from the Molecular Architecture Project, JRDC, Kurume Research Park, Kurume 830, Japan. *Received March 11, 1991*

Abstract: Long-chain derivatives of Kemp's acid formed stable monolayers at the air–water interface, where the carboxylic acid groups produced the cyclic dimer species and served as a molecular cleft for specific binding of nitrogen aromatics and amino acids. The structure of the long-chain substituents was crucial for forming the cyclic dimer. Combinations of FT-IR, XPS, and UV spectroscopies of LB films and surface pressure–area isotherms revealed that substrates of complementary shape and functionality bound to the cleft mainly by hydrogen bonding. Phthalazine formed the 1:2 (substrate/amphiphile) complex, and enhanced binding of phthalazine (binding constant, 30 M^{-1}) compared to that of quinazoline, quinoxaline, and pyridazine was ascribable to the proper location of nitrogen atoms within the molecule as well as smaller solubility in water. A more basic substrate, benzimidazole, bound to the monolayer 5 times more strongly probably in a form of the 1:1 complex. It is remarkable that significant substrate binding was attained even when the host monolayer and the substrates remained in exposure to the aqueous microenvironment. The monolayer of octadecanoic acid was not an effective receptor, implying that the convergent carboxylic acids were the intrinsic element of the molecular recognition.

Introduction

Molecular recognition is a key concept in many areas of chemistry. The use of multiple hydrogen bonding as a means of specific recognition is especially popular in recent years. This interest is derived from its analogy to molecular recognition in the biological system. Rebek and co-workers took advantage of the rigid molecular skeleton of Kemp's triacid to develop a new class of host molecules in which two hydrogen-bonding groups converged to form molecular clefts.[1] Multiple, complementary hydrogen bonding is responsible also for structure-selective extraction of sugars by resorcinol cyclotetramers into CCl_4,[2a] complexation of thymine derivatives with diamidopyridine receptors,[2b,c] and efficient binding of proton acceptors to urea derivatives.[2d]

These host molecules are effective only in organic solvents, due to deteriorating influences of water against host–guest hydrogen bonding. However, sites of molecular recognition in the biological system are usually exposed to the aqueous phase. It is therefore desirable to develop artificial host systems that can recognize guest molecules in direct contact with bulk water.

Organized molecular assemblies on water are uniquely suited for this purpose. Their macroscopic and microscopic organizations are readily characterized by the conventional physicochemical method, and binding functional units can be placed in fixed spatial arrangements in exposure to the aqueous subphase. Specific binding of metal ions by surface monolayers has been reported for host functionalities such as crown ethers,[3] noncyclic crown ethers,[4] and calixarenes.[5] The hydrophobic and electrostatic interactions were mainly responsible for binding by cyclodextrin monolayers.[6] The complementary hydrogen bonding was implied

† Permanent address: Department of Organic Synthesis, Faculty of Engineering, Kyushu University, Hakozaki, Fukuoka 812, Japan.

(1) (a) Rebek, J., Jr.; Askew, B.; Killoran, M.; Nemeth, D.; Lin, F.-T. *J. Am. Chem. Soc.* **1987**, *109*, 2426–2431. (b) Askew, B.; Ballester, P.; Buhr, C.; Jeong, K.-S.; Jones, S.; Parris, K.; Williams, K.; Rebek, J., Jr. *J. Am. Chem. Soc.* **1989**, *111*, 1082–1090. (c) Rebeck, J., Jr. *Top. Curr. Chem.* **1988**, *149*, 189–210. (d) Rebeck, J., Jr. *Acc. Chem. Res.* **1990**, *23*, 399–404.

(2) (a) Aoyama, Y.; Tanaka, Y.; Sugahara, S. *J. Am. Chem. Soc.* **1989**, *111*, 5397–5404. (b) Hamilton, A. D.; Van Engen, D. *J. Am. Chem. Soc.* **1987**, *109*, 5035–5036. (c) Chang, S.-K.; Hamilton, A. D. *J. Am. Chem. Soc.* **1988**, *110*, 1318–1319. (d) Etter, M. C.; Panunto, T. W. *J. Am. Chem. Soc.* **1988**, *111*, 5896–5897.

(3) (a) Zaitsev, S. Yu.; Lutchenko, V. V.; Zubov, V. P. *Biol. Chem. (USSR)* **1983**, *9*, 567–569. (b) Matsumura, H.; Watanabe, T.; Furusawa, K.; Inokuma, S.; Kuwamura, T. *Bull. Chem. Soc. Jpn.* **1987**, *60*, 2747–2750. (c) Yoshida, S.; Okawa, I.; Watanabe, T.; Inokuma, S.; Kuwamura, T. *Chem. Lett.* **1989**, 243–246.

(4) Yanagi, M.; Tamamura, H.; Kurihara, K.; Kunitake, T. *Langmuir* **1991**, *7*, 167–172.

(5) Ishikawa, Y.; Kunitake, T.; Matsuda, T.; Otsuka, T.; Shinkai, S. *J. Chem. Soc., Chem. Commun.* **1989**, 736–737.

0002-7863/91/1513-7342$02.50/0

Scheme I

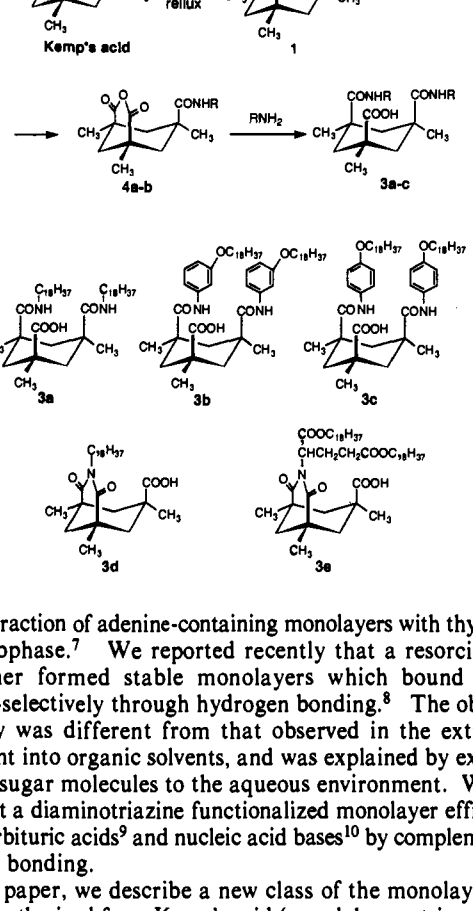

in the interaction of adenine-containing monolayers with thymidine in the subphase.[7] We reported recently that a resorcinol cyclotetramer formed stable monolayers which bound sugars structure-selectively through hydrogen bonding.[8] The observed selectivity was different from that observed in the extraction experiment into organic solvents, and was explained by exposure of bound sugar molecules to the aqueous environment. We also found that a diaminotriazine functionalized monolayer efficiently bound barbituric acids[9] and nucleic acid bases[10] by complementary hydrogen bonding.

In this paper, we describe a new class of the monolayer host that are synthesized from Kemp's acid (a cyclohexanetricarboxylic acid). This system is novel in that two molecules of the monolayer component form a recognition site due to hydrogen bonding. The monolayer formation of these amphiphiles has been briefly described before.[11]

Experimental Section

1. Synthesis of Amphiphiles. Long-chain derivatives of Kemp's acid were synthesized according to Scheme I.

5-(Chloroformyl)-*cis*,*cis*-1,3,5-trimethylcyclohexane-1,3-dicarboxylic Anhydride (1).[12a] Kemp's acid (*cis*,*cis*-1,3,5-trimethylcyclohexane-1,3,5-tricarboxylic acid) was prepared from trimesic acid following the reported procedure:[1a,12] mp 230–234 °C (lit.[1a] mp 240–247 °C, lit.[12a] mp 230–245 °C); IR (KBr, cm^{-1}) 2968 ($\nu_{as\,CH_3}$), 1718 ($\nu_{C=O}$); ^1H NMR (60 MHz, pyridine-d_5) δ 1.53 (d, J = 14 Hz, 3 H, cyclohexyl 3 CH), 1.54 (s, 9 H, 3 CH_3), 3.36 (d, J = 14 Hz, 3 H, cyclohexyl, 3 CH).

Kemp's acid (5.0 g, 19.4 mmol) was refluxed in 60 mL of $SOCl_2$ for 6 h, and extra $SOCl_2$ was evaporated to give white solid of **1** (4.8 g, 96%): mp 268–270 °C (lit.[12a] mp 255–260 °C); IR (KBr, cm^{-1}) 1773 ($\nu_{C=O}$).

3-(Octadecyloxy)aniline (2b). 3-(Acetylamino)phenol (10.0 g, 66.1 mmol), octadecyl bromide (22.1 g, 66.3 mmol), and KOH (5 g, 90 mmol) were dissolved in ethanol (200 mL) and refluxed for 18 h. The precipitate of KBr was filtered from the reaction mixture, and the solvent was removed in vacuo. The residue was dissolved in diethyl ether, washed successively with 1 N NaOH, brine, 1 N HCl, and again with brine, and then dried over $MgSO_4$. Evaporation of solvent in vacuo and recrystallization from acetone gave the white powder of 3-(octadecyloxy)-acetanilide (23.5 g, 88.1%): mp 89–90 °C; IR (KBr, cm^{-1}) 3292 ($\nu_{NH\,amide}$), 2916 ($\nu_{as\,CH_2}$), 2848 ($\nu_{s\,CH_2}$), 1662 ($\nu_{C=O\,amide}$); ^1H NMR (60 MHz, $CDCl_3$) δ 0.87 (t, 3 H, CH_3), 1.26 (s, 32 H, $(CH_2)_{16}$), 2.13 (s, 3 H, $COCH_3$), 3.90 (t, J = 6 Hz, 2 H, OCH_2), 6.43–7.46 (m, 5 H, Ar-H, CONH). Anal. Calcd for $C_{26}H_{45}NO_2$: C, 77.37; H, 11.24; N, 3.47. Found: C, 77.28; H, 11.24; N, 3.39.

3-(Octadecyloxy)acetanilide (10.0 g, 24.8 mmol) was dissolved in 300 mL of ethanol with 10 mL of concentrated HCl, and refluxed for 24 h. The mixture was cooled, the solvent was removed under reduced pressure, and the solids were taken up in $CHCl_3$. The chloroform solution was washed with aqueous saturated $NaHCO_3$ and brine, and dried over $MgSO_4$. After filtration and evaporation of solvent, the residue was recrystallized from acetone to give the white powder of **2b** (7.7 g, 78%): mp 72–73 °C; IR (KBr, cm^{-1}) 3394 ($\nu_{as\,NH\,amine}$), 3298 ($\nu_{s\,NH\,amine}$), 2914 ($\nu_{as\,CH_2}$), 2850 ($\nu_{s\,CH_2}$); ^1H NMR (60 MHz, $CDCl_3$) δ 0.87 (t, 3 H CH_3), 1.23 (s, 32 H, $(CH_2)_{16}$), 3.12 (br s, 2 H, NH_2), 3.84 (t, J = 6 Hz, 2 H, OCH_2), 6.07–6.37 (m, 3 H, Ar-H), 6.78–7.15 (m, 1 H, Ar-H). Anal. Calcd for $C_{24}H_{43}NO$: C, 79.72; H, 11.99; N, 3.87. Found: C, 79.63; H, 11.95; N, 3.81.

4-(Octadecyloxy)aniline (2c). Via the preceding procedure, 4-(acetylamino)phenol (10.0 g, 66.1 mmol) was allowed to react with octadecyl bromide (22.2 g, 66.6 mmol). The following workup gave the white powder of 4-(octadecyloxy)acetanilide (20.5 g, 76.3%): mp 105–106 °C; IR (KBr, cm^{-1}) 3278 ($\nu_{NH\,amide}$), 2916 ($\nu_{as\,CH_2}$) 2848 ($\nu_{s\,CH_2}$), 1658 ($\nu_{C=O\,amide}$); ^1H NMR (60 MHz, $CDCl_3$) δ 0.87 (t, 3 H, CH_3), 1.26 (s, 32 H, $(CH_2)_{16}$), 2.10 (s, 3 H, $COCH_3$), 3.88 (t, J = 6 Hz, 2 H, OCH_2), 6.78 (d, J = 9 Hz, 2 H, Ar-H), 7.32 (br s, 1 H, CONH), 7.34 (d, J = 9 Hz, 2 H, Ar-H). Anal. Calcd for $C_{26}H_{45}NO_2$: C, 77.37; H, 11.24; N, 3.47. Found: C, 77.31; H, 11.28; N, 3.39.

4-(Octadecyloxy)acetanilide (19.4 g, 48.1 mmol) was hydrolyzed with 20 mL of concentrated HCl in ethanol (300 mL). The following workup gave the white powder of **2c** (16.2 g, 93.1%): mp 69–70 °C; IR (KBr, cm^{-1}) 3382 ($\nu_{as\,NH\,amine}$), 3308 ($\nu_{s\,NH\,amine}$), 2914 ($\nu_{as\,CH_2}$), 2848 ($\nu_{s\,CH_2}$); ^1H NMR (60 MHz, $CDCl_3$) δ 0.87 (t, 3 H, CH_3), 1.28 (s, 32 H, $(CH_2)_{16}$), 3.26 (br s, 2 H, NH_2), 3.90 (t, J = 6 Hz, 2 H, OCH_2), 6.61 (d, J = 2 Hz, 4 H, Ar-H). Anal. Calcd for $C_{24}H_{43}NO{\cdot}HCl$: C, 72.41; H, 11.14; N, 3.52. Found: C, 72.35; H, 11.21; N, 3.38.

3,5-Bis(octadecylcarbamoyl)-*cis*,*cis*-1,3,5-trimethylcyclohexane-1-carboxylic Acid (3a). A suspension of **1** (0.8 g, 3.1 mmol) in $CHCl_3$ (50 mL) was added to a solution of octadecylamine (2.5 g, 9.3 mmol) in $CHCl_3$ (100 mL), and the reaction mixture was kept at room temperature for 4 days. The precipitated amine salt was filtered off and the solvent removed in vacuo. The residual oil was dissolved in petroleum ether and cooled to 5 °C for 12 h. The precipitates **4a** were removed, and solvent was removed in vacuo to give a crude solid product. Recrystallization from acetone afforded the white powder of **3a** (0.7 g, 30%): mp 80–83 °C; IR (KBr, cm^{-1}) 3332 ($\nu_{NH\,amide}$), 2918 ($\nu_{as\,CH_2}$), 2848 ($\nu_{s\,CH_2}$), 1704 ($\nu_{C=O\,acid}$), 1632 ($\nu_{C=O\,amide}$); ^1H NMR (400 MHz, $CDCl_3$) δ 0.88 (t, J = 7 Hz, 6 H, 2 CH_3), 1.07 (d, J = 15 Hz, 1 H, CH), 1.10 (d, J = 16 Hz, 2 H, 2 CH), 1.22 (s, 6 H, 2 CH_3), 1.25 (s, 64 H, 2 $(CH_2)_{16}$), 1.34 (s, 3 H, CH_3), 2.86 (t, J = 15 Hz, 3 H, 3 CH), 3.10 (m, 4 H, $NHCH_2$), 6.94 (br s, 2 H, 2 CONH). Anal. Calcd for $C_{48}H_{92}N_2O_4$: C, 75.73; H, 12.18; N, 3.68. Found: C, 75.56; H, 12.09; N, 3.63.

3,5-Bis-[[3-(octadecyloxy)phenyl]carbamoyl]-*cis*,*cis*-1,3,5-trimethylcyclohexane-1-carboxylic Acid (3b). A suspension of **1** (0.8 g, 3 mmol) in $CHCl_3$ (50 mL) was added to a solution of **2b** (3.4 g, 9.3 mmol) in $CHCl_3$ (100 mL) and refluxed for 2 days. The reaction mixture was cooled to room temperature, and the precipitate (the amine salt) was removed. The orgnic layer was washed with aqueous saturated Na_2CO_3, brine, 1 N HCl, and once more with brine, and then dried over $MgSO_4$. After solvent removal in vacuo, the residue (1.6 g) was chromatographed on silica gel (100 g) by using $CHCl_3$ as eluent to give the white solid of **3b** (1.0 g, 33%): mp 107–110 °C; IR (KBr, cm^{-1}) 3288 ($\nu_{NH\,amide}$), 2918 ($\nu_{as\,CH_2}$), 2848 ($\nu_{s\,CH_2}$), 1701 ($\nu_{C=O\,acid}$), 1648 ($\nu_{C=O\,amide}$); ^1H NMR (400 MHz, $CDCl_3$) δ 0.88 (t, J = 7 Hz, 6 H, 2 CH_3), 1.26 (s, 69 H, 2 $(CH_2)_{15}$, 2 CH_3, 3 CH), 1.30 (s, 3 H, CH_3), 1.68 (quin, 4 H, 2 OCH_2CH_2), 2.86 (d, J = 15 Hz, 2 H, 2 CH), 3.02 (d, J = 15 Hz, 1 H, CH), 3.75 (m, 4 H, 2 OCH_2), 6.54 (dd, 2 H, 2 Ar-H), 6.92 (d, J = 8 Hz, 2 H, 2 Ar-H), 7.01 (t, J = 11 Hz, 2 H, 2 Ar-H), 7.06 (s, 2 H, 2 Ar-H), 8.80 (br s, 2 H, 2 CONH). Anal. Calcd for $C_{60}H_{100}N_2O_6$: C, 76.22; H, 10.66; N,

(6) (a) Kawabata, Y.; Matsumoto, M.; Tanaka, M.; Takahashi, H.; Irinatsu, Y.; Tamura, S.; Tagaki, W.; Nakahara, H.; Fukuda, K. *Chem. Lett.* **1986**, 1933–1934. (b) Tanaka, M.; Ishizuka, Y.; Matsumoto, N.; Nakamura, T.; Yabe, A.; Nakanishi, H.; Kawabata, Y.; Takahashi, H.; Tamura, S.; Tagaki, W.; Nakahara, H.; Fukuda, K. *Chem. Lett.* **1987**, 1307–1310.

(7) (a) Ringsdorf, H.; Schlarb, B.; Venzmer, J. *Angew. Chem., Int. Ed. Engl.* **1988**, *27*, 113–158. (b) Kitano, K.; Ringsdorf, H. *Bull. Chem. Soc. Jpn.* **1985**, *58*, 2826–2828.

(8) (a) Kurihara, K.; Ohto, K.; Tanaka, Y.; Aoyama, Y.; Kunitake, T. *Thin Solid Films* **1989**, *179*, 21–26. (b) Idem. *J. Am. Chem. Soc.* **1991**, *113*, 444–450.

(9) Honda, Y.; Kurihara, K.; Kunitake, T. *Chem. Lett.* **1991**, 681–684.

(10) Kurihara, K.; Ohto, K.; Honda, Y.; Kunitake, T. *J. Am. Chem. Soc.* **1991**, *113*, 5077–5079.

(11) A previous account of monolayer formation and dimerization of Kemp's acid derivatives: Ikeura, Y.; Honda, Y.; Kurihara, K.; Kunitake, T. *Chem. Lett.* **1990**, 169–172.

(12) (a) Kemp, D. S.; Petrakis, K. S. *J. Org. Chem.* **1981**, *46*, 5140–5143. (b) Steitz, A., Jr. *J. Org. Chem.* **1968**, *33*, 2978–2979. (c) Newman, M. S.; Lowrie, H. S. *J. Am. Chem. Soc.* **1954**, *76*, 4598–4600.

2.96. Found: C, 76.25; H, 10.68; N, 2.89.

3,5-Bis[[4-(octadecyloxy)phenyl]carbamoyl]-*cis*,*cis*-1,3,5-trimethylcyclohexane-1-carboxylic Acid (3c). **2c** (3.4 g, 9.3 mmol) and **1** (0.8 g, 3.1 mmol) were allowed to react in $CHCl_3$ for 4 days at room temperature as described above. The precipitated amine salt was filtered off, the solvent was removed in vacuo, and the solids were recrystallized three times from benzene, yielding the white powder of **3c** (0.5 g, 17%): mp 137–140 °C; IR (KBr, cm^{-1}) 3270 ($\nu_{NH\ amide}$), 2916 ($\nu_{as\ CH_2}$), 2848 ($\nu_{s\ CH_2}$), 1699 ($\nu_{C=O\ acid}$), 1638 ($\nu_{C=O\ amide}$); ^1H NMR (400 MHz, $CDCl_3$) δ 0.88 (t, J = 7 Hz, 6 H, 2 CH_3), 1.26 (s, 69 H, 2 $(CH_2)_{15}$, 2 CH_3, 3 CH), 1.31 (s, 3 H, CH_3), 1.73 (quin, 4 H, 2 OCH_2CH_2), 2.92 (d, J = 15 Hz, 2 H, 2 CH), 2.99 (d, J = 14 Hz, 1 H, CH), 3.84 (m, 4 H, 2 OCH_2), 6.65 (dd, 4 H, 4 Ar-H), 7.20 (dd, 4 H, 4 Ar-H), 8.69 (br s, 2 H, 2 CONH). Anal. Calcd for $C_{60}H_{100}N_2O_6$: C, 76.22; H, 10.66; N, 2.96. Found: C, 76.30; H, 10.67; N, 2.96.

5-(Octadecylcarbamoyl)-*cis*,*cis*-1,3,5-trimethylcyclohexane-1,3-dicarboxylic anhydride (4a) was isolated from a fraction in column chromatography of **3a** as a white powder: mp 97–101 °C; IR (KBr, cm^{-1}) 3422 ($\nu_{NH\ amide}$), 2918 ($\nu_{as\ CH_2}$), 2850 ($\nu_{s\ CH_2}$), 1797, 1767 ($\nu_{C=O\ unhydride}$), 1647 ($\nu_{C=O\ amide}$); ^1H NMR (60 MHz, $CDCl_3$) δ 0.88 (t, 3 H, CH_3), 1.23 (s, 35 H, $(CH_2)_{16}$, 3 CH), 1.33 (s, 9 H, 3 CH_3), 1.90 (m, 1 H, CH), 2.60 (d, J = 14 Hz, 2 H, 2 CH), 3.13 (m, 2 H, $NHCH_2$), 5.40 (br s, 1 H, CONH). Anal. Calcd for $C_{30}H_{53}NO_4$: C, 73.27; H, 10.86; N, 2.85. Found: C, 73.06; H, 10.85; N, 2.81.

5-[[3-(Octadecyloxy)phenyl]carbamoyl]-*cis*,*cis*-1,3,5-trimethylcyclohexane-1,3-dicarboxylic anhydride (4b) was isolated during the column purification of **3b** as a white powder: mp 137–141 °C; IR (KBr, cm^{-1}), 3370 ($\nu_{NH\ amide}$), 2920 ($\nu_{as\ CH_2}$), 2850 ($\nu_{s\ CH_2}$), 1799, 1768 ($\nu_{C=O\ amide}$), 1654 ($\nu_{C=O\ amide}$); ^1H NMR (400 MHz, $CDCl_3$) δ 0.88 (t, J = 7 Hz, 3 H, CH_3), 1.26 (s, 33 H, $(CH_2)_{15}$, 3 CH), 1.33 (s, 3 H, CH_3), 1.39 (s, 6 H, 2 CH_3), 1.74 (quin, 2 H, OCH_2CH_2), 2.07 (d, J = 14 Hz, 1 H, CH), 2.73 (d, J = 13 Hz, 2 H, 2 CH), 3.93 (t, J = 7 Hz, 2 H, OCH_2), 6.54 (dd, 1 H, Ar-H), 6.77 (dd, 1 H, Ar-H), 7.07 (s, 1 H, CONH), 7.09 (t, J = 2 Hz, 1 H, Ar-H), 7.17 (t, J = 8 Hz, 1 H, Ar-H). Anal. Calcd for $C_{36}H_{57}NO_5$: C, 74.06; H, 9.84; N, 2.40. Found: C, 74.03; H, 9.91; N, 2.39.

2. Surface Pressure–Area (π–A) Isotherms. A computer-controlled film balance (San-esu Keisoku Co., Ltd., model FSD-50) was used for measuring surface pressure as a function of molecular area. The trough size was 600 × 150 mm^2, and the temperature of the aqueous subphase was maintained at 20.0 ± 0.1 °C during the measurement. The concentration of the spreading solution was 10 mg/10 mL $CHCl_3$. After spreading 50 μL of the solution, the monolayer film was incubated for 10 min and then compressed at a rate of 0.4 mm/s. The pH dependence of the π–A isotherms was examined by varying the pH of the subphase with H_2SO_4 or NaOH. The pH of the subphase was monitored before and after π–A measurements. LB films were prepared by using the vertical dipping method at a rate of 20 mm/min. The monolayers were transferred to quartz, CaF_2, or silver-coated (100 nm) glass plates at a surface pressure of 30 mN/m.

3. FT-IR-RAS Measurements. Infrared spectra were obtained on a FT-IR spectrometer (Nicolet, model 710) equipped with a MCT detector (for the RAS, reflection absorption spectroscopy, method) or with a DTGS detector (for the transmission method). All data were collected by the RAS method, unless otherwise stated, at a spectral resolution of 4 cm^{-1}. The p-polarized radiation was introduced on the sample at 80° off the surface normal.

4. XPS Measurements. XPS spectra of the LB films were obtained on an X-ray photoelectron spectrometer (Perking Elmer, ESCA 5300), which was operated at 12 kV–25 mA (300 W) with a Mg Kα X-ray source and at 5 × 10^{-9} Torr. Samples were cooled by liquid N_2, and the sample stage was tilted at different angles (take-off angle) against the analyzer for angle-desolved measurements. Data analysis was carried out by using an Apollo Domain 3500 computer.

Results

Monolayers of Kemp's Acid Derivatives. Figure 1 illustrates the surface pressure–area (π–A) isotherms of compounds **3a–3c** on pure water at 20.0 ± 0.1 °C. These compounds form stable monolayers with collapse pressures of 45 (**3a**), 60 (**3b**), and 30 mN/m (**3c**). We have reported previously that Kemp's acid derivatives of the diamide type (**3a**, **3b**) form more stable monolayers compared to imide ones (**3d**, **3e**).[11] Monolayers of **3d** and **3e** show only the expanded phase with lower collapse pressures of 22 (**3d**) and 31 mN/m (**3e**), whereas monolayers of **3a–3c** give rise to the condensed phase. Higher stability of the amide-type monolayers may be attributed to better packing of alkyl chains in the monolayers. The m-phenylene unit in the side chain of **3b** is especially effective in this respect. The para-substituted derivative **3c** shows a lower collapse pressure than **3b**, though they commonly contain the (octadecyloxy)phenyl unit. CPK molecular model building (Figure 2) implies that the acid dimer of **3c** (see below) is less stable than that of **3b** due to looser packing of alkylphenyl chains in the former. The limiting molecular areas (A_0), areas extrapolated to the zero pressure in the most compressed phase, are 0.59, 0.60, and 0.57 nm^2/molecule for **3a**, **3b**, and **3c**, respectively. These areas are comparable to the molecular cross section of Kemp's acid head group (0.5 nm^2) when the cyclohexane plane orients perpendicular to the water surface (see Figure 2).

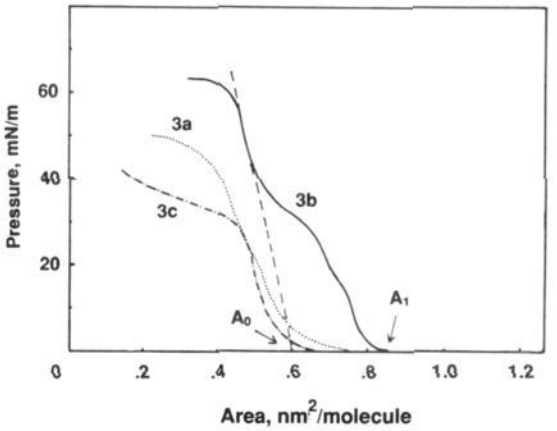

Figure 1. Surface pressure–area (π–A) isotherms of Kemp's acid derivatives (**3a**, **3b**, and **3c**) on pure water at 20.0 ± 0.1 °C. A_0 and A_1 denote the limiting molecular area and the lift-off area of monolayers, respectively.

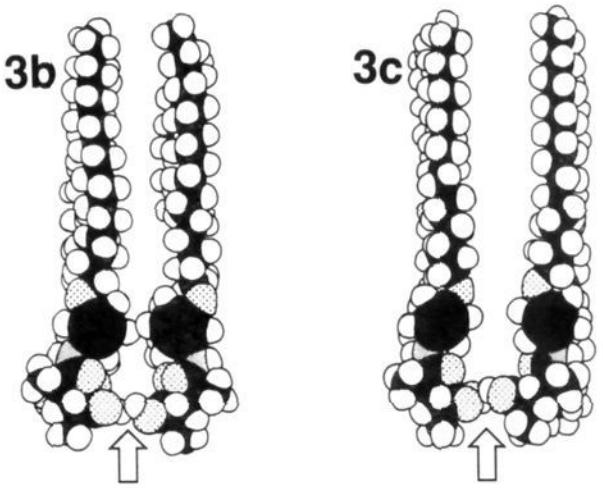

Figure 2. CPK molecular models of cyclic dimers of **3b** (left) and **3c** (right). Arrows point to the carboxylic acid groups. The distance between the two cyclohexane rings of **3b**, estimated from CPK molecular models, is 0.9 nm. Note that a better molecular alignment is attainable with m-phenylene-linked **3b**.

The π–A curve of **3b** hardly changed when the subphase pH was lowered to 2.1 from the pH of pure water (ca. 5.6). An identical curve was observed also at pH 9.0. At higher pH's beyond this value, the isotherm became more expanded due to dissociation of the carboxylic acid. The observed pH dependcence showed that the majority of the acids are in the associated form on pure water, and that the pK_a of **3b** is higher than 9.[13] The extent of expansion also depended on the salt concentration; thus, it was difficult to determine pK_a from π–A curves alone.

Organization of Acid Groups in Monolayers. The head group of these Kemp's acid derivatives possesses the molecular structure that is clearly divided into the hydrophilic surface (side of triaxial

(13) Rebek, J., Jr.; Marshall, L.; Wolak, R.; Parris, K.; Killoran, M.; Askew, B.; Nemeth, D.; Islam, N. *J. Am. Chem. Soc.* **1985**, *107*, 7476–7481.

Table I. FT-IR Absorption Intensities of the LB Films (12 Layers) of **3b** Transferred from the Pure Water Surface[a]

wavenumber, cm^{-1}	assignment	A_T[b]	A_R[c]	A_T/A_R
2918	$\nu_{as\,CH2}$	0.119	0.036	3.3
1703	$\nu_{C=O\,acid}$	0.011	0.027	0.41

[a] Identical spectra were obtained for 1-layer and 12-layer LB films of **3a** and **3b**. Transfer ratios: **3a**, 1.0 for the up-stroke mode and 0.6 for the down-stroke mode; and **3b**, 1.0 for the up-stroke mode and 0.8 for the down-stroke mode. [b] Transmission absorbance. [c] Reflection absorbance.

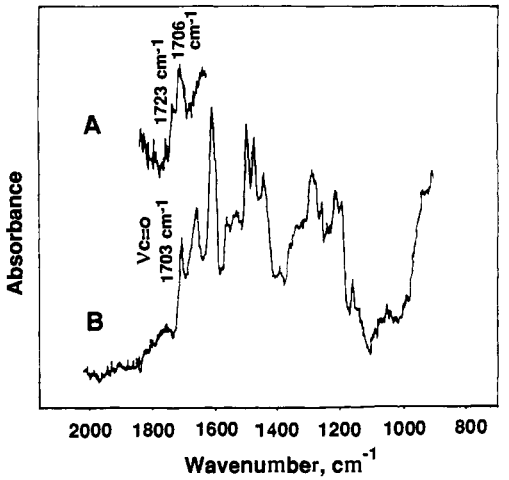

Figure 3. FT-IR reflection absorption spectra of LB films. Sample: (A) one layer of **3a**; (B) one layer of **3b**. Identical spectra were obtained for 1-layer and 12-layer LB films of **3a** and **3b**. Transfer ratios: **3a**, 1.0 for the up-stroke mode and 0.6 for the down-stroke mode; **3b**, 1.0 for the up-stroke mode and 0.8 for the down-stroke mode.

carboxyl groups) and the hydrophobic surface (side of triequatorial methyl groups). The carboxylic acid groups are oriented normal relative to the cyclohexane molecular plane. Therefore, the vertical alignment of the hydrocarbon chain should facilitate hydrogen bonding between two carboxylic acid groups. FT-IR spectroscopy was employed to study these monolayer structures.

LB films of **3b** were prepared on CaF_2 or Ag-coated glass plates by transferring the monolayer from the pure water surface at a surface pressure of 30 mN/m. An FT-IR transmission spectrum of the LB film exhibits strong peaks at 2918 ($\nu_{as\,CH_2}$) and 2848 cm^{-1} ($\nu_{s\,CH_2}$) and a weak peak at 1703 cm^{-1} ($\nu_{C=O\,acid}$), while a reflection absorption spectrum (RAS) of the identical film shows a relatively weak CH_2 band and a stronger C=O peak. Identical spectra are obtainable, independent of the number of layers (1–56 layers).[14] Table I summarizes these peak intensities. Anisotropic LB samples give IR absorption intensities that depend on the orientation of the respective bonds: The transmission method (absorbance, A_T) emphasizes vibrational modes parallel to the film plane, and the RAS method (A_R) emphasizes those perpendicular to the surface.[15] An A_T/A_R value greater than unity (3.3) found for the $\nu_{as\,CH_2}$ band and a smaller value (0.41) for the $\nu_{C=O}$, therefore, indicate that alkyl chains prefer to align perpendicular to the surface (the CH_2 bond direction is parallel to the film plane), while the carbonyl group is oriented parallel to the surface.

The location of the C=O peak of **3b** film (Figure 3B for one-layer film), 1703 cm^{-1}, is very close to that reported for the cyclic dimer of a Kemp's acid, 1705 cm^{-1}.[13] As anticipated from

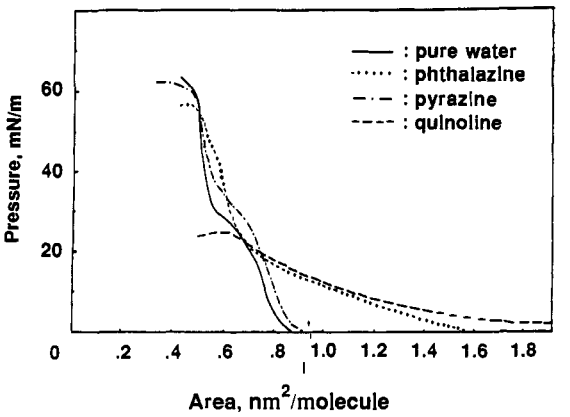

Figure 4. Surface pressure–area isotherms of monolayer **3b** at 20.0 ± 0.1 °C on pure water and on 0.01 M nitrogen aromatics.

Chart I

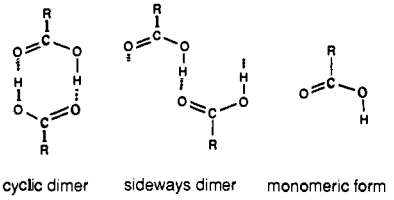

Chart II

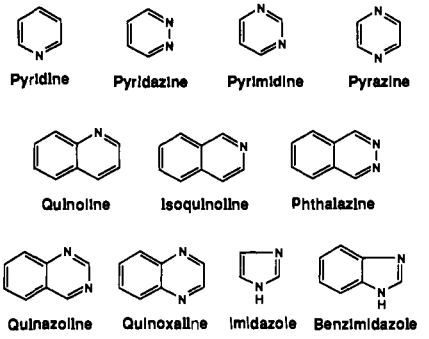

the molecular orientation (see Figure 2), the parallel orientation of the carbonyl group favors the dimer formation in the monolayer. The carbonyl peak in monomeric carboxylic acids should appear at 1760 cm^{-1}. On the other hand, the LB film of **3a** shows a peak at 1706 cm^{-1} with a shoulder at around 1723 cm^{-1} (Figure 3A). The latter absorption is attributable to an acid sideways dimer[16] (Chart I). Thus, monolayer **3a** contains sideways dimers as well as cyclic dimers. It is clear that the *m*-phenylene unit that is additionally included in **3b** promotes precise molecular orientation due to phenyl stacking. The para-substituted derivative **3a** forms a cyclic dimer less efficiently, and its monolayer is less stable. Unfortunately, preparation of LB films of **3c** is difficult owing to its poor transfer; as a result, an FT-IR spectrum is not available for **3c**. The dimeric arrangement of Figure 2 (see also Chart VI) provides an intermolecular cleft that is very similar to those of covalently linked Kemp's acid derivatives. Therefore, binding of hydrogen-bonding substrates to the monolayer was examined in the subsequent experiments.

Binding of Nitrogen Aromatics by Monolayer 3b. Nitrogen aromatics have been suitable candidates for substrates binding in organic media[1a] (Chart II). We therefore studied their binding to monolayer **3b**. The monolayer expands when 0.01 M aqueous phthalazine is used as the subphase (Figure 4). The lift-off area (A_1, defined as the first point on the π–A isotherm where a monolayer shows detectable resistance to compression) increases

(14) Ellipsometric determination (instrument, Gaertner L115B) reveals that the thickness of LB films of **3b** (on a silicon wafer) increases by 56 Å after each deposition cycle (transfer ratios: 0.7 for the down-stroke mode and 1.0 for the up-stroke mode). This value agrees well with the expected thickness of two layers of **3b** (the extended length of **3b** is 34 Å) when the above transfer ratios are taken into account.

(15) Umemura, J.; Kamata, T.; Kawai, T.; Takenaka, T. *J. Phys. Chem.* **1990**, *94*, 62–67.

(16) Davies, G. H.; Yarwood, J. *Thin Solid Films* **1988**, *159*, 461–467.

(17) Briggs, D.; Seah, M. P. *Practical Surface Analysis by Auger and X-ray Photoelectron Spectroscopy*; Wiley: New York, 1983.

Table II. Binding of Nitrogen Aromatics to Monolayer **3b** as Examined by FT-IR and XPX Spectroscopies[a]

substrate in the subphase[b]	pK_a[c]	FT-IR,[d] cm^{-1}	XPS nitrogen/oxygen[e]	XPS nitrogen/carbon
none (calcd)			0.33	0.033
none (exptl)			0.31	0.031
pyridine	5.2	no change	0.32	0.034
pyridazine	2.2	1703 (slightly↓)	0.33	0.035
pyrimidine	1.3	no change	0.30	0.033
pyrazine	~1	no change	0.32	0.035
quinoline	4.88	1703↓	0.33	0.036
isoquinoline	5.38	1703↓	0.35	0.036
phthalazine	3.4	1703↓, 1678↑	0.41 (1/4.3)	0.041
			0.43 (1/3.4)[f]	
quinazoline	3.5	no change	0.30	0.037
quinoxaline	0.56	no change	0.34	0.035
imidazole	6.95	1703↓, 1666↑	0.40 (1/5)	0.040
benzimidazole	5.53	1703↓, 1669↑	0.50 (1/2)	0.047
			0.55 (1/1.5)[g]	

[a] LB films (12 layers) were transferred to silver-coated (100 nm) glass plates at a surface pressure of 30 mN/m except for aqueous quinoline and isoquinoline (20 mN/m). [b] 0.01 M substrates unless otherwise stated. [c] Albert, A. In *Physical Methods in Heterocyclic Chemistry*; Katritzky, A., Ed.; Academic Press: New York, 1963; Vol. I. [d] Arrows, ↑ and ↓, indicate increase and decrease, respectively, in IR intensities. [e] The figures in parentheses are molar ratios of substrate to **3b**. [f] 0.05 M phthalazine. [g] 0.03 M benzimidazole.

from 0.84 nm^2/molecule on pure water to 1.55 nm^2/molecule. The limiting area A_0 increases also from 0.60 nm^2/molecule on pure water to 0.72 nm^2/molecule. The expansion depends on the phthalazine concentration, and is observable at concentrations above 0.001 M. Similar changes occur on aqueous solutions of other nitrogen aromatics, though the extent of expansion varies depending on substrates. Examples of the isotherm change are shown in Figure 4. Because these π–A isotherms are not identical in shape, two indices (A_1 and A_0) are used to describe the effect. The lift-off area A_1 increases in the order H_2O (0.84 nm^2/molecule) < pyrazine (0.90) ≈ pyridazine (0.90) < pyridine (1.19) < imidazole (1.29) < quinoxaline (1.47) ≈ benzimidazole (1.49) ≈ phthalazine (1.53) < quinoline (>1.9). The limiting area A_0 increases in the order H_2O (0.60 nm^2/molecule) ≈ pyrazine (0.60) ≈ pyridine (0.60) < pyridazine (0.64) ≈ quinoxaline (0.64) < imidazole (0.66) < benzimidazole (0.71) ≈ phthalazine (0.71). The expansion is not caused by the pK_a change alone, since direct correlation is not found between the expansion effect of a substrate and its pK_a value (see Table II). The isotherm does not specify origins of the substrate–monolayer interaction; therefore, analytical methods such XPS, UV–vis and FT-IR spectroscopies are required to characterize the interaction.

Spectroscopic Determination of Nitrogen Aromatics Bound to Monolayer 3b. X-ray photoelectron spectroscopy (XPS) is a convenient means to monitor changes in the chemical composition of LB films upon substrate binding to monolayers. Monolayer **3b** was transferred onto Ag-coated (1000 Å) slide glasses from subphases of pure water and aqueous substrates. An XPS spectrum of an LB film (12 layers of **3b**) prepared from pure water (take-off angle, 45°) shows peaks assigned to C_{1s} (284.6 eV), N_{1s} (397.9 eV), and O_{1s} (531.6 eV).[16] No peak was detected at 367.9 eV (Ag_{3d}), thus contribution of the substrate emission on the oxygen peak being negligible. A bare Ag-coated glass without the LB deposition has peaks for both Ag_{3d} and O_{1s}. The spectrum does not change at higher take-off angles. The peak areas give atomic compositions of the sample after correction of relative sensitivity factors. The nitrogen/oxygen and nitrogen/carbon ratios thus obtained are 0.31 and 0.031 (±5%), and agree well with the theoretical values of 0.33 and 0.033, respectively. An XPS spectrum of an LB film of **3b** deposited from 0.01 M aqueous phthalazine shows an enhanced N_{1s} peak (N/O = 0.41, N/C = 0.041), indicating incorporation of phthalazine into the monolayer. The observed N/O ratio corresponds to the 1:4 molar ratio of phthalazine to **3b**. The N/O ratio increases only slightly to 0.43 at a higher phthalazine concentration of 0.05 M.

Binding of other nitrogen aromatics from their 0.01 M aqueous solutions was similarly examined, and results are summarized in Table II. The XPS data clearly demonstrate selective binding of certain substrates to **3b** monolayer. The N/O ratio of 0.5 found for the benzimidazole case corresponds to 2:1 molar ratio of **3b** to benzimidazole. It increases to 0.55 (**3b**/benzimidazole, 1.5/1) at a higher benzimidazole concentration of 0.03 M. The benzimidazole binding is more efficient than that of phthalazine, suggesting that the modes of binding of these substrates are different. It is interesting that the increase in the N/O ratios is related to that in the limiting area, A_0, in the π–A isotherm. Imidazole and benzimidazole, which show large A_0 values (0.66 and 0.71 nm^2/molecule, respectively), raise the nitrogen concentration in LB films, whereas pyridine and pyridazine, which do not shift A_0, are hardly incorporated in the films. This correlation does not hold necessarily. Quinoline does expand the monolayer considerably, but its incorporation as inferred from the N/O ratio is small. Quinoline may not form a stable complex with the compressed monolayer, although its interaction with the monolayer is obvious.

Binding of benzimidazole (a chromophoric substrate) can be monitored by UV absorption spectroscopy. The absorption spectrum of monolayer **3b** deposited from pure water exhibits a peak at 282 nm (absorbance, 0.0056), which is assigned to the absorption of the phenyl group of **3b** (molar extinction coefficient, 6800 in EtOH). An LB film of **3b** (one layer) transferred onto a quartz plate from 0.01 M aqueous benzimidazole displays an additional absorption. A difference spectrum between these two LB films shows a peak at 243 nm (absorbance, 0.0053), which agrees well with the absorption of benzimidazole in water. Nonspecific incorporation of benzimidazole is corrected by measuring absorbance (0.0031 at 243 nm) of a monolayer-free plate dipped in 0.01 M benzimidazole (under otherwise the same conditions as that of monolayer transfer). After this background correction, the molar ratio of **3b** to benzimidazole in the film is determined to be 1.9:1, in close agreement with the XPS result of 2:1.

The interaction of these nitrogen aromatics with the monolayer was further investigated by FT-IR spectroscopy. LB films of **3b** were prepared on Ag-coated glass plates from aqueous phthalazine subphases and from pure water. Their FT-IR spectra are shown in Figure 5. An LB film of **3b** from 0.001 M aqueous phthalazine gives a spectrum identical to that from pure water. A new band appears at 1678 cm^{-1} at the expense of the original carbonyl absorption at 1703 cm^{-1}, when the phthalazine concentration is increased to 0.005 and 0.05 M. A powder mixture of **3b** and phthalazine in KBr does not reveal any shift of this carbonyl band. The ionized carboxyl group shows a characteristic absorption between 1610 and 1550 cm^{-1},[18] which is far from 1678 cm^{-1}. Hydrogen bond adducts (not polarized) of carboxylic acids and nitrogen aromatic bases usually possess the C=O peak close to that of the acid dimer, and its wavelength depends on the nature of donors and acceptors.[19] Therefore, one may conclude that the shift from 1703 to 1678 cm^{-1} arises from hydrogen bonding of phthalazine with the carboxylic group of Kemp's acid with accompanying dissociation of the original acid dimer.

Table II includes FT-IR changes of LB films due to binding of nitrogen aromatics. The LB films that contain imidazole or benzimidazole show carbonyl peak shifts from 1703 cm^{-1} to 1666 and 1669 cm^{-1}, respectively. This implies formation of acid–base adducts by hydrogen bonding similar to that of phthalazine.[19] Quinoline and isoquinoline (XPS analysis shows their moderate incorporation in the LB films) causes decreases in the peak intensity at 1703 cm^{-1} to some extent, while pyridine, quinoxaline, and quinazoline do not cause any change in the IR spectrum. A 0.01 M pyridazine solution does not alter the spectrum noticeably,

(18) Ballamy, L. J. *The Infra-red Spectra of Complex Molecules*, 3rd ed.; John Wiley & Sons: New York, 1975.

(19) (a) Johnson, S. L.; Rumon, K. A. *J. Phys. Chem.* **1965**, *69*, 74–86. (b) Lindemann, R.; Zundel, G. *J. Chem. Soc., Faraday Trans. 2* **1977**, *73*, 788–803.

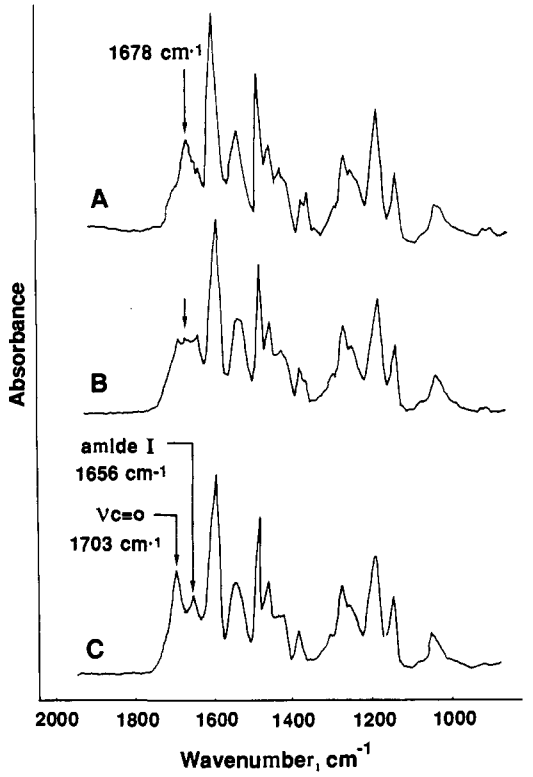

Figure 5. FT-IR reflection absorption spectra of LB films of **3b** transferred from various subphases. Subphase: (A) 0.05 M phthalazine; (B) 0.005 M phthalazine; (C) pure water. LB films (12 layers) were transferred to silver-coated (100 nm) glass plates at a surface pressure of 30 mN/m. Transfer ratios: 1.0 for the up-stroke mode and 0.8 for the down-stroke mode.

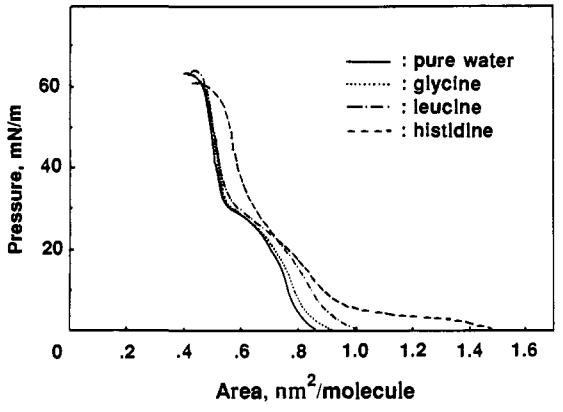

Figure 6. Surface pressure–area isotherms of monolayer **3b** at 20.0 ± 0.1 °C on pure water and on 0.01 M aqueous amino acids.

but the C=O intensity begins to decrease when its concentration is raised to 0.1 M. These XPS and IR data establish that monolayer **3b** binds nitrogen aromatics selectively.

Binding of Amino Acids to Monolayer 3b. Because of the zwitterionic character, amino acids form only weak complexes with lone pair donors, and their recognition is generally performed either in acidic pH or at the other end of pH. Recently, Rebek et al. have demonstrated specific recognization of aromatic amino acids by Kemp's acid dimer at neutral pH.[20] As described above, a cleft similar to the dimeric receptor, which consists of two convergent carboxylic groups, is formed in monolayer **3b**.

The surface pressure–area isotherm of **3b** expands when the subphase contains various amino acids at 0.01 M (Figure 6). The isotherms are analogous in shape to each other; therefore, the expansion effect may be expressed in terms of A_0 alone. The A_0

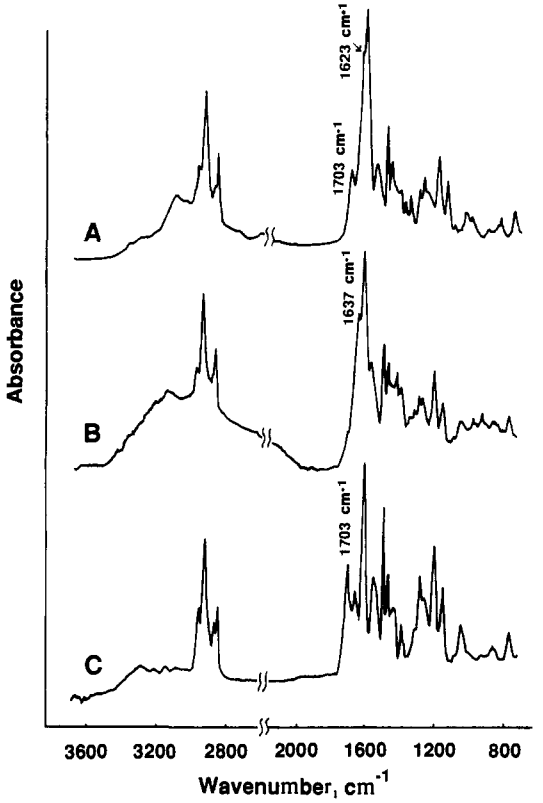

Figure 7. FT-IR reflection absorption spectra of LB films of **3b** transferred from various subphases. Sample: (A) 12-layer LB film from 0.01 M alanine; (B) 1-layer film from 0.01 M histidine; (C) 12-layer film from 0.01 M alanine. LB films were transferred to silver-coated (100 nm) glass plates at a surface pressure of 30 mN/m.

value increases in the order H_2O (A_0 = 0.84 nm^2/molecule) < alanine (1.01) < leucine (1.06) < phenylalanine (1.34) < histidine (1.52) < tryptophan (1.59). Hydrophobic amino acids phenylalanine and tryptophan expand the monolayer more efficiently. On the other hand, it is interesting to note that hydrophilic histidine causes a similar extent of expansion.

The interactions between the monolayer and amino acids, as implied by the π–A isotherm, can be examined by FT-IR spectroscopy (RAS method). An LB film of **3b** prepared from 0.01 M histidine[21] shows a broad peak at 3400–2200 cm^{-1} (ν_{NH3^+}) and a peak at 1637 cm^{-1} ($\delta_{as\ NH_3^+}$), which are characteristic peaks of histidine[18] (Figure 7B). The peak at 1703 cm^{-1} ($\nu_{C=O\ diacid}$) disappears, indicating the binding of histidine through interaction with the carboxyl group. The interaction can be ionic (with $-NH_3^+$) and/or hydrogen bonding (with the imidazole ring). In fact, IR data of Table II suggest that monolayer **3b** binds imidazole and benzimidazole by hydrogen bonding. The $\delta_{as\ NH_3}$ peak of histidine and the $\nu_{aromatic}$ peak of **3b** (1610 cm^{-1}) overlap with the $\nu_{C=O}$ of the carboxylic acid (ionic CO_2H, 1560–1600 cm^{-1}; hydrogen-bonded CO_2H, 1650–1700 cm^{-1}), and its is difficult to interpret the observed peaks in terms of specific ionic and/or hydrogen-bonding interactions. Tryptophan causes a similar spectral change, though the peak at around 3000 cm^{-1} is weaker and the $\delta_{as\ NH_3^+}$ peak appears at 1653 cm^{-1}.

In the case of amino acids that do not possess basic side chains (alanine, leucine, and phenylalanine), IR spectra undergo changes in even more complicated manners. An FT-IR spectrum of an LB film prepared from aqueous alanine is shown in Figure 7A. A broad peak at around 3000 cm^{-1} (ν_{NH3^+}) and a peak at 1620 cm^{-1} ($\delta_{as\ NH3^+}$) prove incorporation of alanine in the film. The intensity of the $\nu_{C=O\ diacid}$ peak at 1703 cm^{-1} is lessened only partially, though; it suggests that the carboxylic acid group is

(20) Rebek, J., Jr.; Askew, B.; Nemeth, D.; Parris, K. *J. Am. Chem. Soc.* **1987**, *109*, 2432–2434.

(21) Only one layer of **3a** or **3b** was transferrable from 0.01 M aqueous histidine or tryptophan, whereas multilayer deposition was possible from aqueous glycine, alanine, or phenylalanine.

Table III. Interaction of Nitrogen Aromatics and Amino Acids with Monolayers of **3a**, **3b**, and **5** as Studied by FT-IR Spectra of LB Films[a]

substrates in the subphase (0.01 M)	FT-IR[b]		
	3b	**3a**	**5**
phthalazine	1703 ($\nu_{C=O}$) ↓ 1678 ($\nu_{C=O}$) ↑	no change	no change
imidazole	1703 ($\nu_{C=O}$) ↓ 1666 ($\nu_{C=O}$) ↑	no change no change	no change no change
benzimidazole	1703 ($\nu_{C=O}$) ↓ (complete loss) 1669 ($\nu_{C=O}$)	1707 ($\nu_{C=O}$) ↓ (70% loss) 1645 ($\nu_{C=O}$) ↑	1706 ($\nu_{C=O}$) ↓ (30% loss) 1557 (ν_{COO^-}) ↑
histidine	1703 ($\nu_{C=O}$) ↓ 1637 ($\delta_{NH_3^+}$) ↑	1707 ($\nu_{C=O}$) ↓ 1638 ($\delta_{NH_3^+}$) ↑	
alanine	1703 ($\nu_{C=O}$) (slight loss) 1620 ($\delta_{NH_3^+}$) ↑	1707 ($\nu_{C=O}$) (slight loss) 1632 ($\delta_{NH_3^+}$) ↑	no change
tryptophan	1703 ($\nu_{C=O}$) (slight loss) 1653 ($\delta_{NH_3^+}$) ↑	1707 ($\nu_{C=O}$) (slight loss) 1654 ($\delta_{NH_3^+}$) ↑	no change

[a] LB films (12 layers) were transferred to silver-coated (100 nm) glass plates at a surface pressure of 30 mN/m except for histidine and tryptophan (1 layer).[20] [b] Peak positions (cm^{-1}) and intensity changes. Arrows, ↑ and ↓, indicate increase and decrease, respectively, in IR intensities.

responsible for the binding of alanine. The smaller change of the $\nu_{C=O}$ peak may be attributed to the dimer formation between the carboxylic acid of **3b** and that of amino acids (see below). LB films obtained from aqueous leucine and phenylalanine similarly exhibit characteristic IR peaks of the amino acid.

Binding of Nitrogen Aromatics and Amino Acids by Monolayers of 3a and Octadecanoic Acid. The results described above clearly show specific binding of nitrogen aromatics and amino acids to the monolayer of **3b**. It is interesting to know whether there is any structural uniqueness of **3b** that is related to this specific interaction. We, therefore, investigated binding of these substrates to monolayers of **3a** and octadecanoic acid (**5**), both of which bear the carboxylic acid group. LB films of **3a** and **5** were prepared from pure water and from aqueous solutions (0.01 M) of nitrogen aromatics (phthalazine, imidazole, and benzimidazole) and amino acids (alanine, tryptophan, and histidine), and subjected to FT-IR spectroscopy. As summarized in Table III, marked differences are found for binding characteristic of these monolayers.

Although the structure of monolayer **3a** is similar to that of **3b** with regard to cyclic dimer formation and A_0, subphase phthalazine does not alter the FT-IR spectrum of a **3a** LB film. No change is observed with an FT-IR spectrum of monolayer **5** obtained from aqueous phthalazine. Similarly, aqueous imidazole does not provide any evidence of binding to monolayers of **3a** or **5**, in spite of the fact that 0.2 equiv of imidazole is incorporated into monolayer **3b**. On the other hand, benzimidazole, which shows the highest affinity to monolayer **3b** (50 mol % binding), is bound to both the monolayers **3a** and **5**. This results in a decrease in the $\nu_{C=O}$ peak intensity at 1707 cm^{-1} by 70% and an increase of peak intensity at 1645 cm^{-1} in the case of **3a**. The decrease is ca. 30% in the case of **5**, and is accompanied by appearance of a new peak of the carboxylate anion at 1557 cm^{-1}.[22] The nature of hydrogen bonds that are formed between nitrogen bases and carboxylic acids depends on the pK difference between bases and acids: When the difference exceeds a certain value, the hydrogen bond becomes more ionic and the ν_{COO^-} peak (1550–1610 cm^{-1}) appears.[18] Apparently, a less polarized complex is formed between benzimidazole and **3a** and **3b**, but the ion pair form is more probable in the case of monolayer **5**.

Interactions of amino acids with monolayers of **3a** and **5** were also studied. Binding of alanine, tryptophan, and histidine to monolayer **3a** is supported by appearance of their IR characteristic peaks ascribed to the $\nu_{as\,NH_3^+}$ mode: 1632 cm^{-1} for alanine, 1654 cm^{-1} for tryptophan, and 1638 cm^{-1} for histidine. The relative intensity of the $\nu_{C=O}$ peak at 1707 cm^{-1} changes only slightly by aqueous alanine and tryptophan, but more by histidine: $I(\nu_{C=O})/I(\nu_{CH_2})$ = 0.3 (pure water, alanine), 0.25 (tryptophan), 0.15 (histidine). On the other hand, the LB film of **5** prepared from aqueous alanine or tryptophan shows no characteristic peaks of amino acids.

Chart III

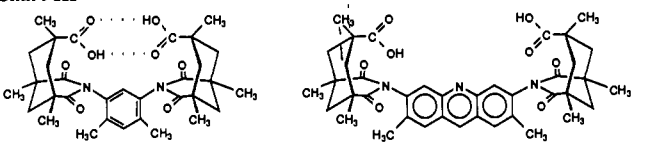

6 7

Chart IV

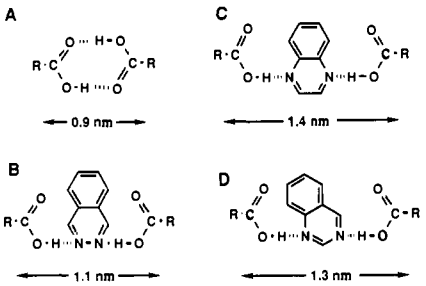

Discussion

Molecular Design of Binding Site. The preceding results clearly demonstrate that nitrogen aromatics as well as amino acids are specifically (in selectivity and/or in modes of binding) bound to the monolayer of **3b** from the aqueous subphase. Hydrogen bonding between substrates and the carboxylic acid groups of the monolayer must be responsible for this specific interaction. The binding efficiency depends highly on orientation and organization of the acid groups in monolayers. Molecular receptors that have been prepared from Kemp's acid[7,22] possess binding sites composed of two covalently linked carboxylic acid groups. In the present monolayer system, formation of the cyclic dimer species is attained by appropriate association of the two carboxylic acid groups. The *m*-phenylene derivative of Kemp's acid (**3b**) is particularly suitable for this purpose. Its monolayer exhibits the $\nu_{C=O}$ peak at 1703 cm^{-1}. The structural resemblance of that of Rebek's receptor **6** (the $\nu_{C=O}$ peak at 1705 cm^{-1}) is clear[13] (Chart III). This convergent orientation of the acid groups in monolayer **3b** produces high affinities and selectivities in guest binding. Compound **3a** that forms the sideways dimer along with the cyclic dimer in monolayer displays much less affinities and selectivities toward guest molecules. Therefore, it is apparent that the presence of the *m*-phenylene unit is crucial in producing proper orientation of the adjacent carboxylic acid units. The carboxylic acid unit in an LB film of octadecanoic acid (**5**) has been reported to form a cyclic dimer between the adjacent layers: $\nu_{C=O}$ at 1706 cm^{-1}.[23] This type of dimerization requires an orientation of the carboxylic acid perpendicular to the layer plane. Thus, monolayer **5** cannot form a convergent binding site such as **3** at the air–water interface, and shows an inferior binding capability.

Modes of Substrate Binding. Specificity and efficiency of incorporation of substrates from the aqueous subphase are determined by the modes of hydrogen bonding, the extent of electrostatic interaction, and substrate distribution at the interface. The contribution of these factors should depend on particular classes of substrates.

Among the less basic nitrogen aromatics, the location of the nitrogen atoms within the molecule and the solubility of substrates in water appear to control the binding behavior. An interesting

(22) The relative intensity of the $\nu_{C=O}$ (1707 cm^{-1} for **3a** and 1706 cm^{-1} for **5**) and ν_{CH_2} (2922 cm^{-1} for **3a** 2917 cm^{-1} for **5**) peak changes from 0.3 (pure water subphase) to 0.1 (benzimidazole subphase) for an LB film of **3a**, and from 0.7 (pure water) to 0.5 (benzimidazole) for an LB film of **5**.

(23) Kimura, F.; Umemura, J.; Takenaka, T. *Langmuir* **1986**, *2*, 96–101.

Chart V

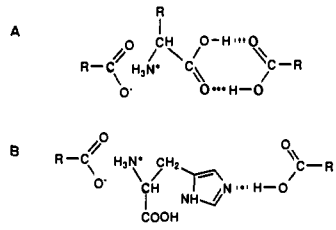

comparison can be made among the binding behavior of three isomeric substrates: phthalazine, quinazoline, and quinoxaline. The binding efficiency is not correlated with the basicity, because phthalazine (pK_a, 3.4) is bound better than quinazoline (pK_a, 3.5). Instead, the location of the two nitrogen atoms exerts greater influences. These substrates may be bound to monolayer **3b** through nonpolarized hydrogen bonding, as confirmed for phthalazine by FT-IR data (Figure 5). Probable models of dual hydrogen bonding of the three substrates are illustrated in Chart IV. The distance between the two cyclohexane planes of Kemp's acid in monolayer **3b** is estimated to be 0.9 nm (±5%) from the CPK model building (Chart IV, complex A). The limiting molecular area in the π–A isotherm (0.60 nm^2) is close to the molecular cross section (0.5 nm^2) of the head group (Kemp's acid unit). This result endorses the validity of the estimate based on the CPK molecular model.

The distance between the two cyclohexane rings upon substrate binding would be estimated by adding 0.9 nm (cyclohexane separation without substrate binding) to the van der Waals distance of the two nitrogen atoms of phthalazine (0.29 nm), quinoxaline (0.56 nm), and quinazoline (0.49 nm). Phthalazine is bound to monolayer **3b** effectively, but quinoxaline and quinazoline are not, as indicated by the data of Table II. The molecular area A_0 of **3b** increases by 17% upon 50% binding of phthalazine (Figure 1). The 50% binding in the manner of Chart IV, complex B, should cause 11% expansion. The agreement is satisfactory. A greater separation of the cyclohexane rings would lead to lessened packing of the monolayer component. This type of binding would not occur readily, consistent with poor binding of quinoxaline and quinazoline.

A similar situation may as well be found among pyridazine, pyrimidine, and pyrazine. However, pyridazine is bound to monolayer **3b** inefficiently, as indicated by a slight decrease in the C=O peak at 1703 cm^{-1}. Apparently, these substrates are too soluble in water, and hydrogen bonding, if effective, will not be sufficient enough to produce a detectable amount of bound substrates.

Imidazole and benzimidazole are nitrogen aromatics of greater basicity. This property affects their binding pattern. Benzimidazole binds to monolayer **3b** most efficiently. The molar ratio of **3b** to benzimidazole in an LB film prepared from 0.03 M benzimidazole (near saturation) is determined by XPS to be 1.5:1. This figure is greater than the stoichiometric ratio of 2:1 that is expected from the binding mode of Chart IV. Therefore, benzimidazole forms a 1:1 hydrogen-bonded complex with **3b** at least partially, probably because its greater basicity enhances the stability of the complex. The binding of benzimidazole to three monolayers (**3a**, **3b**, and **5**) is rather undiscrimating, compared with that of other nitrogen aromatics. The lack of specificity again suggests that the mode of benzimidazole binding is not the dual hydrogen bonding of Chart IV. Lesser association of imidazole relative to benzimidazole is rationalized by higher solubility of imidazole of water.

Binding of amino acids occurs in more complicated manners. Since the monolayer of octadecanoic acid (**5**), which does not possess the convergent carboxylic acid unit, fails to bind amino acids, two-point interaction appears to exist between amino acids and monolayers **3a** and **3b**: See Chart V. The FT-RI data clearly indicate the presence of the NH_3^+ group in bound amino acids. Therefore, one of the carboxylic acids in the cyclic dimer forms carboxylate–ammonium ion pairs with the amino acid. Except for histidine, the second interaction is in the form of the cyclic

Chart VI

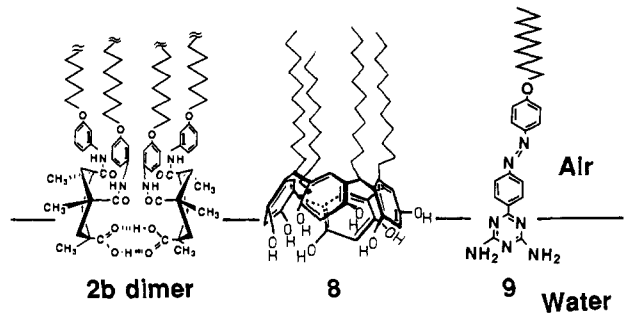

carboxylic acid dimer, since the $\nu_{C=O}$ peak of the cyclic dimer (at 1703 cm^{-1} for **3b** and at 1707 cm^{-1} for **3a**) is lowered only partially or slightly. However, when histidine is bound, the $\nu_{C=O}$ peak is lost totally or almost completely. This suggests that the second carboxylic acid unit in the receptor site forms a hydrogen bond with the imidazole ring. The acid–base interaction is energetically more favorable than the acid–acid interaction (formation of the cyclic dimer).

It is noteworthy that binding of amino acids is less specific than that of (less basic) nitrogen aromatics. Simultaneous formation of two hydrogen bonds as in phthalazine binding (Chart IV, complex A) requires highly specific arrangements of host and guest molecules. The spatial requirement is much less rigorous in the case of ion pair formation with amino acids (Chart V).

Formation of Receptor Sites by Covalent Linkage and Molecular Assembly. Molecular recognition by monolayers of derivatives of Kemp's acid resembles that by covalently linked, dimeric counterparts[7,22] in many respects. Multiple hydrogen bonding and ion pair formation are responsible for specific binding in both systems. The lipophilic property of substrate molecules leads to enhanced binding in both systems.

The crucial convergent structure is produced by propert covalent linking in Rebek's systems. The length and rigidity of the connector portion have been used to regulate the binding specificity. The stacking interaction of aromatic substrates with aromatic connectors can strengthen the host–guest interaction. In the monolayer system, the receptor site is produced spontaneously by molecular assembly. We had not anticipated highly specific binding, since simple molecular assembly would not produce well-defined receptor sites. Our finding described in this paper was therefore a pleasant surprise. The convergent carboxylic acid unit can be formed by proper alignments of the alkyl chains in monolayers. Substrate molecules are bound in such a way as not to disturb the original monolayer assemblage too seriously. This conclusion implies that the pattern of selectivity is varied by changing the manner of side-chain organization. Designed molecular assemblage may give rise to a range of specificity comparable to that of covalently linked counterpart.

The molecular association constant of a covalently linked Kemp's acid (**7**) in $CDCl_3$ is reported to be ca. 10^3 M^{-1} for nitrogen aromatics containing two nitrogen atoms and 1.5×10^4 M^{-1} for benzimidazole.[1a] The association constant of monolayer **3b** is estimated to be 30 M^{-1} for phthalazine and 150 M^{-1} for benzimidazole, by assuming Langmuir adsorption.[24] The monolayer values are smaller by a factor of ca. 100, partly due to higher competition of substrate binding with cyclic dimer formation. The distance of two carboxyl groups is greater than that of a stable dimer in receptor **7**. The difference in the association constants of 2 orders of magnitude is surprisingly small, if we take into account the fact that the substrate molecules bound to the monolayer receptor remain exposed to water. It is known that hydrogen bonding of substrate molecules with solvent molecules produce large detrimental effects in their binding affinities toward hydrogen-bonding receptors.[25,26] The calculated dissociation

(24) Barrow, G. M. *Physical Chemistry*, 2nd ed.; McGraw-Hill: New York, 1966.

(25) Hamilton, A. D. In *Advances in Supramolecular Chemistry*; Gokel, G. W., Ed.; JAI: Greenwich, CT, London, 1990; Vol. 1, pp 1–64.

energy of the hydrogen bond in vacuo ranges from −3.1 to −19 kcal·mol^{-1}; whereas hydrogen bond energies in an enzyme–substrate complex range from −0.5 to −1.5 kcal·mol^{-1} for uncharged donors and acceptors. The smaller energies in solutions are believed to be due in large part to the effect of water.[25] The association constant of a diamidepyridine receptor with a barbiturate decreases from 3000 M^{-1} in CCl_4 to 155 M^{-1} in $CDCl_3$.[26] Therefore, the large binding constants we observed in the presence of water (in the magnitude of 100 M^{-1}) may be attributed to unique features of the air–water interface. As mentioned in the Introduction, the monolayer of a resorcinol cyclotetramer (**8**) binds monosaccharides structure-selectively.[8] A diaminotriazine functionalized monolayer (**9**) effectively binds barbituric acids[9] and nucleic acid bases[10] by complementary hydrogen bonding. Strong solvation of these polar substrates by water does not prohibit their efficient hydrogen bonding with the functional monolayers on water. This unique feature may arise from rigid alignment of the receptor site on water and/or anisotropic microenvironments near the interface, as discussed before.[8] We do not know the exact answer yet.

(26) Schneider, H.-J.; Juneja, R. K.; Simova, S. *Chem. Ber.* **1989**, *122*, 1211–1213.

Registry No. 1, 79410-29-0; **2b**, 135365-30-9; **2c**, 65972-30-7; **3a**, 128208-38-8; **3b**, 135365-33-2; **3c**, 135365-34-3; **4a**, 135365-31-0; **4b**, 135365-32-1; 3-(acetylamino)phenol, 621-42-1; octadecyl bromide, 112-89-0; 4-(acetylamino)phenol, 103-90-2; 4-(octadecyloxy)acetanilide, 73722-04-0; 4-(octadecyloxy)aniline, 4105-89-9; octadecylamine, 124-30-1; pyridine, 110-86-1; pyridazine, 289-80-5; pyrimidine, 289-95-2; pyrazine, 290-37-9; quinoline, 91-22-5; isoquinoline, 119-65-3; phthalazine, 253-52-1; quinazoline, 253-82-7; quinoxaline, 91-19-0; imidazole, 288-32-4; benzimidazole, 51-17-2; alanine, 56-41-7; leucine, 61-90-5; phenylalanine, 63-91-2; histidine, 71-00-1; tryptophan, 73-22-3; octadecanoic acid, 57-11-4.

Intramolecular Palladium-Catalyzed Trimethylenemethane Cycloadditions: Initial Studies

Barry M. Trost,*,† Timothy A. Grese, and Dominic M. T. Chan

Contribution from the Department of Chemistry, Stanford University, Stanford, California 94305, and Department of Chemistry, University of Wisconsin, Madison, Wisconsin 53706. *Received March 4, 1991*

Abstract: The potential application of [3 + 2] cycloadditions to polycarbocycle construction is considerably enhanced by the ability to perform such reactions intramolecularly. The feasibility of such processes is explored in the context of Pd-catalyzed cycloadditions of 2-[(trimethylsilyl)methyl]allyl carboxylates, wherein trimethylenemethane (TMM) precursor fragment (donor) and the electron-deficient olefin (acceptor) is joined by a tether of simple methylene groups of 3, 4, 5, and 8 members. Several versatile synthetic routes to these substrates were developed. 2-Bromo-3-(trimethylsilyl)propene proves to be a key reagent for construction of the donor portion. Acceptors bearing esters, cyano groups, and especially sulfones have been examined. The diastereoselectivity of the reaction has been explored both in terms of ring juncture and the diastereofacial selectivity with respect to an oxygen substituent at the allylic position of the acceptor. Excellent cycloadditions to give the bicyclo[3.3.0]octyl and bicyclo[4.3.0]nonyl systems are observed, whereas larger rings cannot be obtained in this series. The choice of catalyst proves critical, the most useful being either tetrakis(triphenylphosphine)palladium and DPPE or, more generally, triisopropyl phosphite and palladium acetate. The first cycloaddition of a 1,1-dialkylated TMM precursor, which fails in intermolecular cases, has been observed in this intramolecular series to give a bridgehead-substituted bicycle. A rationale for the observed diastereoselectivity is presented.

Ring construction constitutes a continuing major challenge in synthetic organic chemistry. Processes that involve forming more than one bond enhance synthetic efficiency. The tremendous success of the Diels–Alder reaction attests to this fact. New dimensions of selectivity evolve by extending these intermolecular processes to intramolecular ones. In the case of Diels–Alder reactions, questions of regio-, diastereo-, and enantioselectivity have been of particular interest.[1] Much less work has been done in the related 1,3-dipolar cycloadditions; nevertheless, the growing body of literature on their intramolecular versions reveal many unique aspects associated with tethering the two reaction partners.[2]

Carbocyclic versions of the [3 + 2] cycloaddition have emerged largely within the recent past.[3-13] Their intramolecular versions have remained virtually untapped. Of the few studies that exist, the intramolecular cycloadditions of allyl cations,[4] 1,3-diyls,[9] and methylenecyclopropanes[11] stand out.

Our development of a [3 + 2] cycloaddition via the intermediacy of trimethylenemethane palladium complexes (TMM–PdL_2)[12] demands an exploration of the feasibility of an intramolecular version. The geometrical constraints established by the tether may lead to competing reactions, notably protodesilylation. To the extent that cycloaddition will occur, the question of regioselectivity arises. In this paper, we report our initial studies that establish the feasibility of intramolecular [3 + 2] cycloadditions via TMM–PdL_2 intermediates.[14]

† Address correspondence to this author at Stanford University.

(1) For some recent reviews, see: Brieger, G.; Bennett, J. N. *Chem. Rev.* **1980**, *80*, 63. Kametani, T.; Nemoto, H. *Tetrahedron* **1981**, *37*, 3. Fallis, A. G. *Can. J. Chem.* **1984**, *62*, 183. Ciganek, E. *Org. React.* **1984**, *32*, 1. Weinreb, S. *Acc. Chem. Res.* **1985**, *18*, 16. Taber, D. F. *Intramolecular Diels–Alder and Alder Ene Reactions*; Springer-Verlag: Berlin, 1984. Salakhov, M. S.; Ismailov, S. A. *Russ. Chem. Rev.* (*Engl. Transl.*) **1986**, *55*, 145. Craig, D. *Chem. Soc. Rev.* **1987**, *16*, 187. Roush, W. R. *Adv. Cycloaddit.* **1990**, *2*, 91. Carruthers, W. *Cycloaddition Reactions in Organic Synthesis*; Pergamon Press: Oxford, 1990.

(2) For some reviews, see: Padwa, A. *Angew. Chem., Int. Ed. Engl.* **1976**, *15*, 123. Oppolzer, W. *Angew. Chem., Int. Ed. Engl.* **1977**, *16*, 10. Confalone, P. N.; Huie, E. M. *Org. React.* **1988**, *36*, 1. Terao, Y.; Aono, M.; Achiwa, K. *Heterocycles* **1988**, *27*, 981. Padwa, A.; Schoffstall, A. M. *Adv. Cycloaddit.* **1990**, *2*, 1.

(3) For allyl anions in [3 + 2] cycloadditions, see: Hudlicky, T. *Chem. Rev.* **1989**, *89*, 1467. Kauffmann, T. *Top. Curr. Chem.* **1980**, *92*, 109. Also see: Beak, P.; Burg, D. A. *J. Org. Chem.* **1989**, *59*, 1647. Padwa, A.; Yeske, P. E. *J. Am. Chem. Soc.* **1988**, *110*, 1617. Bunce, R. A.; Wamsley, E. J.; Pierce, J. D.; Shellhammer, A. J., Jr.; Drumright, R. E. *J. Org. Chem.* **1987**, *52*, 464.

(4) For allyl cations in [3 + 2] cycloadditions, see: Mann, J. *Tetrahedron* **1986**, *42*, 4611. Remaiah, M. *Synthesis* **1984**, 529. Noyori, R.; Hayarawa, Y. *Org. React.* **1983**, *29*, 169. Hoffmann, H. M. R. *Angew. Chem., Int. Ed. Engl.* **1984**, *23*, 1. Noyori, R. *Acc. Chem. Res.* **1979**, *12*, 61. Also see: Gray, B. D.; McMillan, C. M.; Miller, J. A.; Ullah, G. M. *Tetrahedron Lett.* **1987**, 689. Ipaktschi, J.; Lauterbach, G. *Angew. Chem., Int. Ed. Engl.* **1986**, *25*, 354.

0002-7863/91/1513-7350$02.50/0